energies

MDPI

Article

Numerical Investigation on Mixture Formation and Injection Strategy Optimization in a Heavy-Duty PFI Methanol Engine

Zhancheng Dou [1,2], Xiaoting Xu [3], Changhui Zhai [1,2], Xiaoxiao Zeng [1,2], Kui Shi [1,2], Xinbo Wu [1,2], Yi Liu [3], Yunliang Qi [3,*] and Zhi Wang [3]

[1] Weichai Power Co., Ltd., Weifang 261001, China
[2] State Key Laboratory of Engine and Powertrain System, Weifang 261001, China
[3] School of Vehicle and Mobility, Tsinghua University, Beijing 100084, China; xxt23@mails.tsinghua.edu.cn (X.X.)
* Correspondence: qiyunliang@tsinghua.edu.cn

Abstract

Methanol is a liquid fuel with high oxygen content and the potential for a closed-loop carbon-neutral production cycle. To investigate the mixture formation and combustion characteristics of a heavy-duty Port Fuel Injection (PFI) methanol engine, a three-dimensional numerical simulation model was established using the CONVERGE 3.0 software. Multi-cycle simulations were performed to analyze the influence of wall film dynamics on engine performance. The results indicate that the "adhesion–evaporation" equilibrium of the intake port wall film determines the in-cylinder mixture concentration. Due to the high latent heat of vaporization of methanol, severe wall-wetting occurs during the initial cycles, causing the actual fuel intake to lag behind the injection and leading to an overly lean mixture and misfire. Regarding injection strategies, the open valve injection (OVI) strategy utilizes high-speed intake airflow to reduce wall adhesion and improve fuel transport efficiency compared to closed valve injection. OVI refers to the fuel injection strategy that injects fuel into the intake port during the intake valve opening phase. The open valve injection strategy (e.g., SOI −500° CA) demonstrates distinct superiority over closed valve strategies (SOI −200°/−100° CA), achieving a 75% reduction in wall film mass. The long injection duration and early phasing allow the high-speed intake airflow to carry fuel directly into the cylinder, significantly minimizing wall film accumulation and avoiding the "fuel starvation" observed in closed-valve strategies. Additionally, OVI fully utilizes methanol's latent heat to generate an intake cooling effect, which lowers the in-cylinder temperature and helps suppress knock. Furthermore, a dual-injector strategy is proposed to balance spatial atomization and rapid fuel transport, which achieves a 66.7% increase in the fuel amount entering the cylinder compared with the original strategy. This configuration effectively resolves the fuel induction lag, achieving stable combustion starting from the first cycle.

Keywords: methanol engine; port fuel injection; fuel film

Check for updates

Academic Editors: Constantine D. Rakopoulos and Andrea Reverberi

Received: 2 December 2025
Revised: 21 December 2025
Accepted: 5 January 2026
Published: 7 January 2026

Copyright: © 2026 by the authors. Licensee MDPI, Basel, Switzerland. This article is an open access article distributed under the terms and conditions of the Creative Commons Attribution (CC BY) license.

1. Introduction

Under the stringent constraints of global climate change mitigation and the imperative for energy security, the decarbonization of the heavy-duty transportation sector has become a critical priority. Methanol, as a liquid fuel with high oxygen content and the potential for a closed-loop carbon-neutral production cycle (e.g., "electro-methanol" from green

hydrogen and captured CO_2), is increasingly recognized as a pragmatic alternative to diesel for heavy-duty internal combustion engines (ICEs) [1–3]. Possessing a high research octane number (RON > 108) and a high laminar flame speed, methanol enables engines to operate at higher compression ratios with improved thermal efficiency while significantly reducing nitrogen oxides and particulate matter emissions compared to conventional fossil fuels [4–6]. While direct injection (DI) strategies have gained traction, Port Fuel Injection (PFI) remains a highly attractive solution for retrofitting existing heavy-duty platforms due to its cost-effectiveness, simplicity, and extended time for fuel-air mixing.

However, the application of methanol in PFI engines presents unique thermophysical challenges that distinguish it from gasoline or natural gas. The most prominent barrier is methanol's high latent heat of vaporization (1103 kJ/kg, approximately three times that of gasoline) combined with its low saturation vapor pressure [7]. During engine startup or transient load changes, fuel droplets injected into the intake port struggle to evaporate instantaneously. Instead, they tend to impinge upon the intake port walls and the back of the intake valves, forming a substantial liquid wall film [8]. This severe "wall-wetting" phenomenon disrupts the fuel transport dynamics, causing the mass of fuel entering the cylinder to lag significantly behind the injected mass (fuel induction lag) [9]. Recent experimental studies by Li et al. [10] and Yuan et al. [11] have highlighted that this instability leads to severe cycle-to-cycle variations, lean mixture misfires during the initial cycles, and elevated emissions of unburned hydrocarbons and formaldehyde due to incomplete combustion. Wang et al. [12] conducted an experimental investigation into the cyclic variation characteristics of diesel–methanol dual fuel (DMDF) combustion on a methanol-fumigated diesel engine. The results demonstrated that the combustion stability of DMDF was comparable to that of neat diesel combustion under high-load conditions, whereas under low-load conditions, the magnitude of cyclic variations in DMDF combustion increased significantly, and such variations were more sensitive to the quantity of fumigated methanol. Chen et al. [13] carried out an experimental study on diesel–methanol dual fuel (DMDF) combustion in a turbocharged inline four-cylinder diesel engine. Their findings indicated that the engine exhibited a lower degree of unevenness when methanol injectors were installed at the intake manifold or the distal end of the inlet duct, compared with the setup where the injectors were fixed at the proximal end of the inlet duct. Mousavi et al. [14] modified a 6-cylinder, 13 L diesel engine to adopt a dual-fuel supply mode with port-fuel-injected (PFI) methanol and direct-injected (DI) diesel, where diesel served as the pilot fuel, and conducted relevant experimental investigations. The results indicated that increasing the methanol energy fraction under all test conditions intensifies the differences between the in-cylinder pressure traces of the two cylinders.

To decipher the complex multiphase flow mechanisms within the intake port and optimize mixture formation, computational fluid dynamics has become an indispensable tool. However, standard steady-state simulations often fail to capture the transient evolution of the wall film. Accurate prediction requires a rigorous coupling of spray atomization, droplet-wall interaction, and evaporation models. Liu et al. [15] emphasized that the formation and evaporation of the wall film are not instantaneous but require multiple engine cycles to reach a dynamic equilibrium. Consequently, multi-cycle numerical simulations are essential to accurately predict the "adhesion–evaporation" balance [16]. Furthermore, the geometric complexity of the intake assembly plays a critical role. Yuan et al. [11] visualized spray impingement on curved valves, revealing that the velocity loss and splashing behavior on curved surfaces differ fundamentally from flat-plate models, necessitating specific calibration of impingement models for heavy-duty engines.

Optimizing the injection strategy is the primary pathway to mitigate wall-wetting and enhance methanol engine performance. Existing research has extensively explored

injection phasing and injector orientation. Regarding phasing, early work by Li et al. [17] established basic correlations between timing and emissions. More recently, Zhu et al. [18] and Wei et al. [19] investigated the thermodynamic impact of injection timing, finding that open valve injection (OVI) significantly reduces wall film accumulation by utilizing high-speed intake airflow for entrainment. Crucially, Zhu et al. [18] demonstrated that OVI leverages methanol's high latent heat to cool the intake charge directly, thereby lowering the temperature at the start of compression and thermodynamically suppressing knock—an advantage that is diminished in closed valve injection (CVI) where evaporation heat is primarily drawn from the port walls. In terms of spatial arrangement, Tian et al. [20] investigated oblique injection angles, finding that utilizing the "double collision" effect against the port wall and valve stem can aid atomization. However, a fundamental trade-off remains: placing the injector far upstream promotes pre-evaporation but increases wall-wetting [21], while placing it close to the valve improves transient response but may sacrifice spatial atomization quality [22].

Despite these advances, few studies have systematically addressed the coupling mechanism between injector axial position and injection phasing under multi-cycle transient conditions to resolve the "cold start" misfire dilemma. To address this gap, this study establishes a calibrated three-dimensional numerical model of a heavy-duty PFI methanol engine. Multi-cycle simulations are performed to investigate the dynamic equilibrium of wall film transport. The study quantitatively compares the fuel transport efficiency and thermodynamic cooling effects of open versus closed valve injection and proposes a dual-injector injection strategy. The findings aim to provide a reference for eliminating fuel induction lag and achieving stable combustion.

2. Methodology

Figure 1 shows the overall structural diagram of the test bench, and Figure 2 presents the cloud map of the temperature field distribution of the cylinder head. It can be clearly seen from the cloud map that the area around the combustion chamber forms a distinct high-temperature concentration zone due to its direct exposure to the high-temperature thermal shock of fuel gas, and its temperature is significantly higher than that of other parts of the cylinder head. Three-dimensional simulations were performed using the CONVERGE 3.0 software. The main performance and technical parameters of the engine are listed in Table 1. The geometry of the engine's combustion system is illustrated in Figure 3.

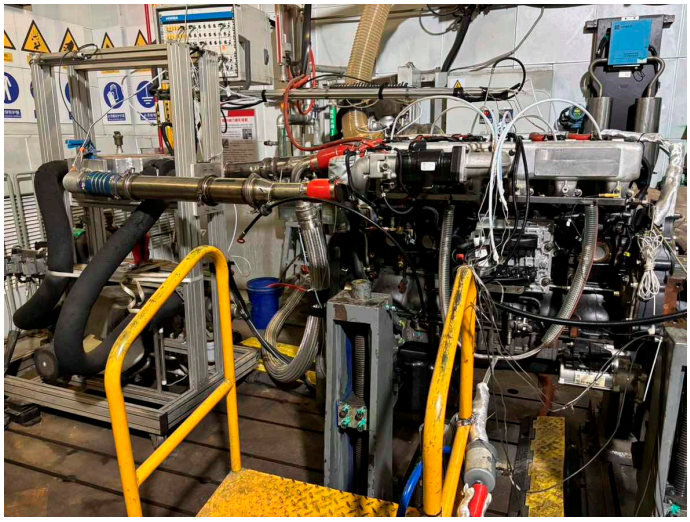


Figure 1. Engine test bench.

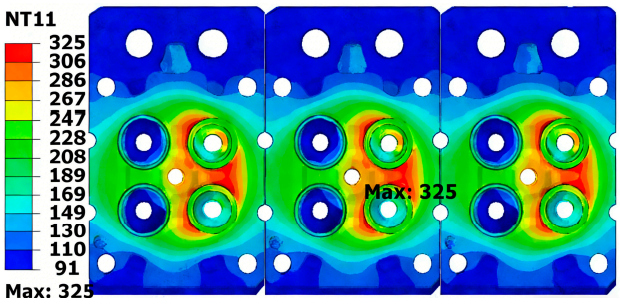


Figure 2. Temperature field contour map of the cylinder head.

Table 1. Engine specifications.

Parameter	Value
Bore	131 mm
Stroke	160 mm
Intake Valve Opening	−373° CA
Intake Valve Closing	−153° CA
Ignition Energy	90 mJ
Compression Ratio	12.5
Excess Air Coefficient	1

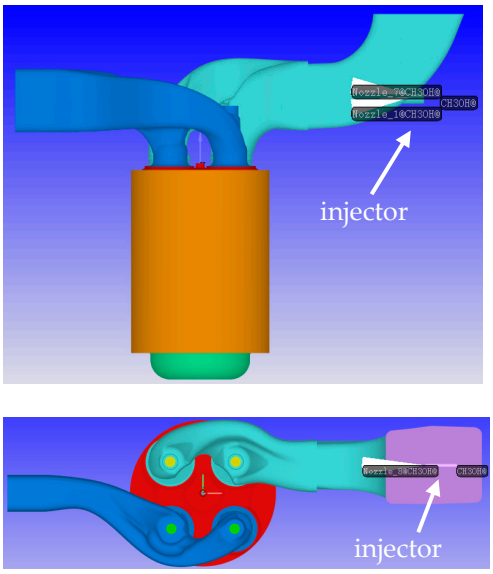


Figure 3. Geometry of the engine's combustion system.

A base grid size of 4 mm was employed, with a minimum embedding grid size of 0.5 mm. Adaptive Mesh Refinement (AMR) was applied to refine key areas such as the methanol injector, spark plug, and intake valves. The Renormalized Group (RNG) k-ε turbulence model within the Reynolds Averaged Navier–Stokes (RANS) framework was selected for the calculations. The SAGE model was adopted to solve the combustion process using a detailed chemical reaction mechanism developed by Chang et al. [23]. The Han and Reitz model was selected to calculate heat transfer. The simulations in this study cover multiple engine cycles, with 0° CA defined as the compression top dead center (TDC).

This study focuses on the numerical simulation of a Port Fuel Injection (PFI) methanol engine. In engines employing this injection strategy, a considerable portion of injected droplets inevitably impinges upon and adheres to the inner wall of the intake port, forming a substantial liquid fuel film. In addition to wall-deposited fuel, a portion of the spray remains suspended in the intake port and cannot enter the cylinder once the intake valve

closes. Since the fuel distribution in the intake port determines the uniformity of the in-cylinder air–fuel ratio, the accurate construction and calibration of the PFI injection model are essential prerequisites for reliable full-engine simulations. Capturing this complex process requires the coordinated tuning of multiple interacting sub-model parameters.

Notably, the calibration of the PFI model cannot be performed in isolation. Considering that the film evaporation rate significantly alters in-cylinder combustion boundary conditions, the physical wall film model and the chemical combustion process must be treated as a coupled system during calibration. Furthermore, from the perspective of physical mechanisms, the accumulation and evaporation of the fuel film in the intake port are not instantaneous; establishing a dynamic equilibrium of mass exchange often requires several working cycles. Therefore, to ensure the reliability of the calibration results, multi-cycle numerical simulations were conducted.

Figure 4 presents a comparison between the simulated pressure and HRR curves of Cycle-4 and experimental values. The shapes of the simulated and experimental data show good agreement. Furthermore, the simulated HRR curve matches the experimental data well in terms of peak magnitude, peak phase, and heat release duration, indicating that the calibrated numerical model satisfies the requirements for engine performance prediction.

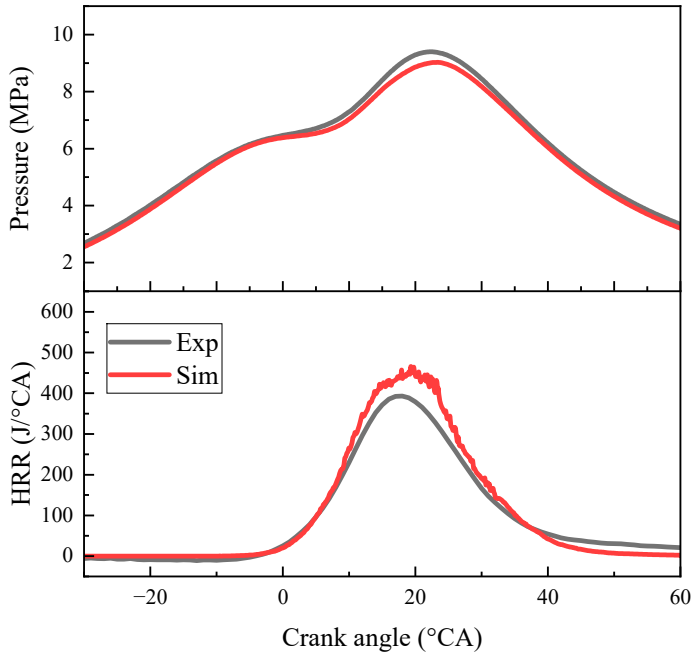


Figure 4. Comparison of the simulated in-cylinder pressure and HRR of Cycle-4 with the experiment.

3. Results

3.1. Multi-Cycle Numerical Simulation and Combustion Stabilization Process

Initially, the methanol injection, evaporation, and combustion processes were calculated using default spray and wall models. The results indicated that, even after multiple cycles, the majority of the injected methanol remained within the intake port and failed to enter the cylinder to form a mixture of sufficient concentration, as shown in Figure 5. The parameters significantly affecting fuel spray and impingement include the RT Model size constant (governing spray atomization), the Rebound Weber number and Separation constant (governing wall interaction), and the intake port wall roughness. Consequently, this study focused on calibrating these parameters for the methanol injection and evaporation process. Based on extensive parametric studies, the final selected parameter values are presented in Table 2.

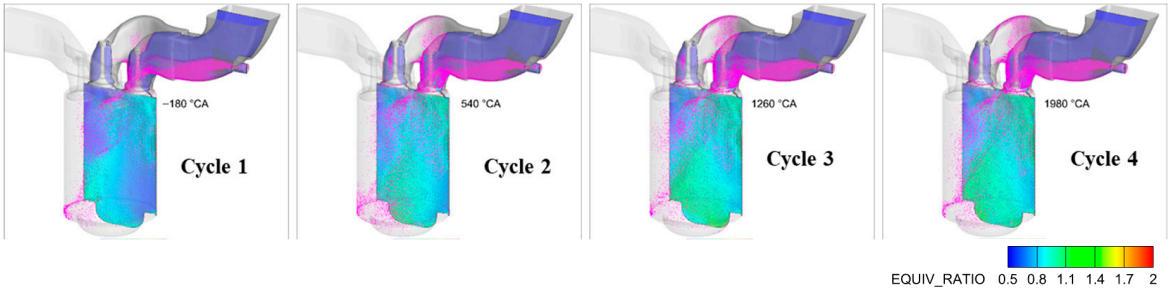


Figure 5. Spatial distribution of methanol droplets at the bottom dead center for 4 consecutive cycles.

Table 2. Model parameters.

Parameter	Value
RT Model size constant	0.1
Rebound Weber number	50
Separation constant	80
Wall roughness	2.6×10^{-4} m

Based on the calibrated parameters, further research was carried out under the operating conditions detailed in Table 3. Figure 6 presents the cylinder pressure and heat release rate (HRR) curves obtained through numerical simulation at the engine's rated power point.

Table 3. Engine operating condition for numerical simulation.

Parameter	Value
Speed	1900 rpm
Intake pressure	0.237 MPa
Intake temperature	338.4 K
Fuel injection pressure	0.5 MPa
Fuel injection duration	−310~203° CA
EGR ratio	25%
Spark timing	−12.6° CA ATDC

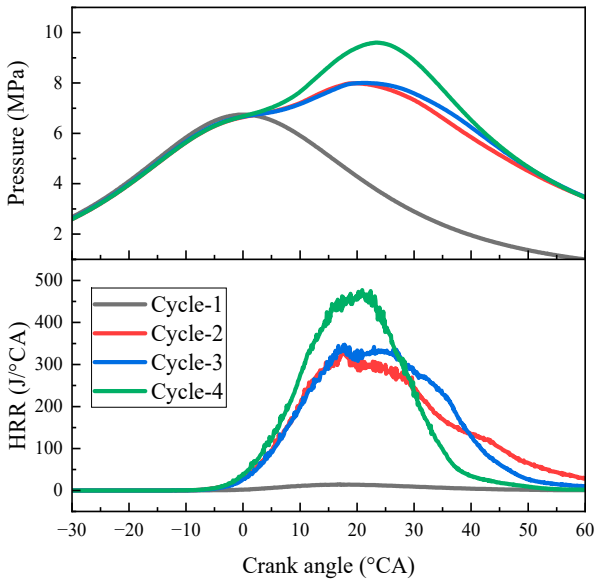


Figure 6. Cylinder pressure and heat release rate of four consecutive cycles.

As shown in Figure 6, for the first cycle (Cycle-1), the peak of the cylinder pressure is extremely low, only slightly exceeding the motoring pressure. However, the corresponding heat release rate exhibits a weak but identifiable peak near the compression TDC. Simultaneously, the in-cylinder temperature field (Figure 7a) indicates that the spark plug successfully ignited the mixture, forming a flame front that propagated slowly outward. Therefore, Cycle-1 does not represent a complete misfire but rather a slow combustion process. This phenomenon is attributed to the fact that Cycle-1 represents the initial injection cycle during engine startup. Due to the high latent heat of vaporization of methanol, when fuel is injected onto the cold intake port wall, the vast majority adheres as a liquid film, with only a small amount entering the cylinder with the air (Figure 8). This results in an extremely lean in-cylinder mixture ($\lambda > 1.5$, as shown in Figure 7b). Under these conditions, flame propagation speed is abnormally slow and flame temperature is low, preventing the flame from effectively filling the combustion chamber before the expansion stroke; thus, the contribution to cylinder pressure elevation is negligible.

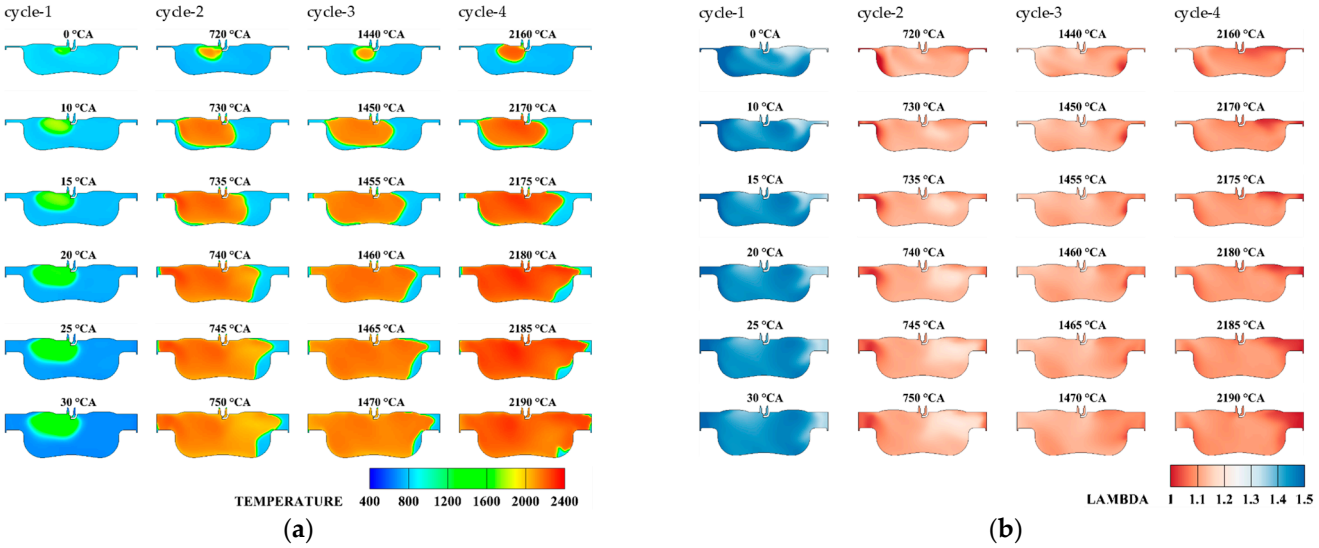


Figure 7. Cycle-to-cycle variations in in-cylinder fields over four consecutive cycles: (**a**) temperature distributions at selected crank angles; (**b**) corresponding λ distributions at the same crank angles.

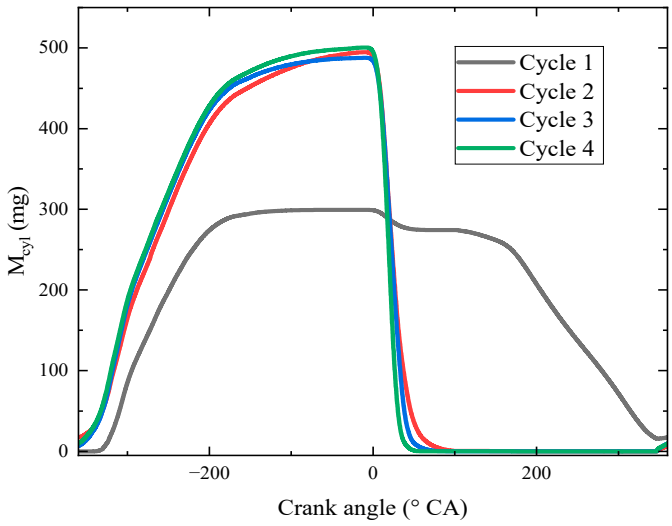


Figure 8. In-cylinder methanol mass evolution for four consecutive engine cycles. (M_{cyl}: the instantaneous mass of methanol entering the cylinder).

In the second cycle (Cycle-2, Figure 6), the combustion state improves significantly. The cylinder pressure shows a sharp rise, reaching a peak of 8 MPa, and the HRR curve presents a high, concentrated peak (approx. 300 J/° CA). This indicates that Cycle-2 achieved rapid and relatively more complete combustion. This improvement occurs because the intake port wall film formed in Cycle-1, along with residual droplets in the intake port, begins to partially evaporate during the cycle interval and the intake process of Cycle-2. Superimposed with the newly injected fuel vapor, this leads to a substantial increase in the fuel mass entering the cylinder compared to Cycle-1 (Figure 8). The mixture distribution confirms this: the average in-cylinder λ decreases significantly (Figure 7b), falling within the effective flammability range of methanol. Consequently, the flame propagation shows that the mixture is quickly ignited and develops into a high-speed turbulent flame, filling almost the entire combustion chamber within approximately 30° CA (by 750° CA) (Figure 7a).

The performance of the third cycle (Cycle-3) is relatively similar to that of Cycle-2. In the fourth cycle (Cycle-4), the peak cylinder pressure (10 MPa) and peak HRR (approx. 480 J/° CA) reach the highest values in the sequence (Figure 6). Physically, this suggests that after the accumulation of the previous cycles, the adhesion and evaporation of the wall film and spatial droplets in the intake port reach an optimized dynamic equilibrium, resulting in a more ideal mixture concentration entering the cylinder. The mixture distribution shows that the in-cylinder mixture approaches the stoichiometric ratio (Figure 7b); this superior condition promotes faster flame propagation and more complete energy release.

3.2. Injection Phasing

This section investigates the influence of different Start of Injection (SOI) timings. The injection duration was set to 513° CA, the same as the previous cases in Section 3.1. The in-cylinder combustion and mixture formation processes were comparatively analyzed under three strategies: SOI −500° CA (early injection before and during the intake stroke), −200° CA (injection at the end of the intake stroke), and −100° CA (injection after intake valve closing).

The evolution curves of cylinder pressure and heat release rate (Figure 9) clearly illustrate the decisive role of injection phasing on engine performance. Under the −500° CA strategy, the engine demonstrates optimal characteristics, achieving rapid and robust combustion starting from Cycle-1, with peak cylinder pressure and HRR maintaining high stability in subsequent cycles. In contrast, delaying the injection timing to −200° CA and −100° CA severely deteriorates the combustion conditions of the first cycle. For the −200° CA condition, Cycle-1 experiences a nearly complete misfire, and Cycle-2 shows only weak heat release; relatively normal combustion is not established even by Cycle-4. For the −100° CA condition, due to the excessively retarded injection, the peak cylinder pressure and HRR are the lowest, resulting in the poorest combustion performance.

The fundamental reason for these discrepancies lies in the degree of matching between the injection timing and the intake valve timing, which directly determines fuel induction efficiency and wall film formation. As shown in the methanol cylinder induction mass curve (Figure 10), under the −500° CA condition, the early start and long duration (513° CA) allow the injection process to cover the entire intake stroke (−373° CA to −153° CA). Consequently, most of the fuel is carried directly into the cylinder by the high-speed intake airflow, manifested as a high methanol induction mass even in Cycle-1. Conversely, in the −200° CA and −100° CA conditions, the intake valve closes at −153° CA, meaning most of the fuel is injected while the valve is closing or closed. This results in insufficient fuel intake during the current cycle, causing an extremely lean in-cylinder mixture and triggering misfire. Fuel from the retarded injection primarily contributes to wall film formation, entering the cylinder through evaporation only in subsequent cycles.

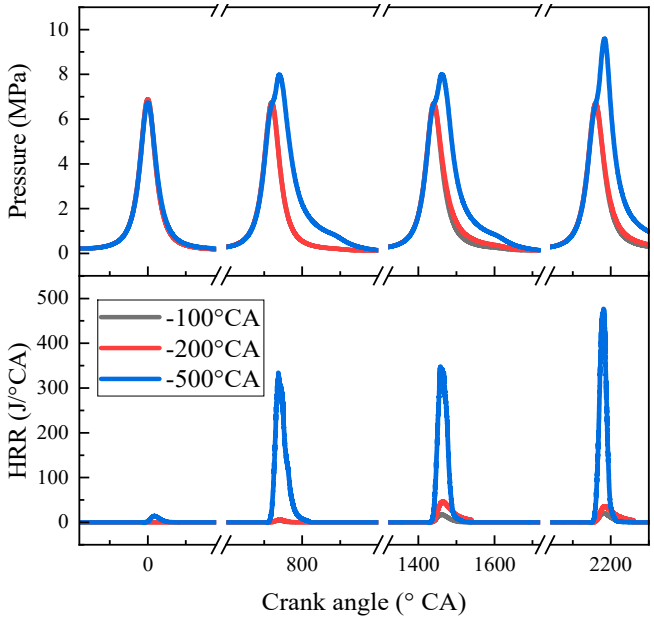


Figure 9. Cylinder pressure and heat release rate of four consecutive cycles under different injection timings.

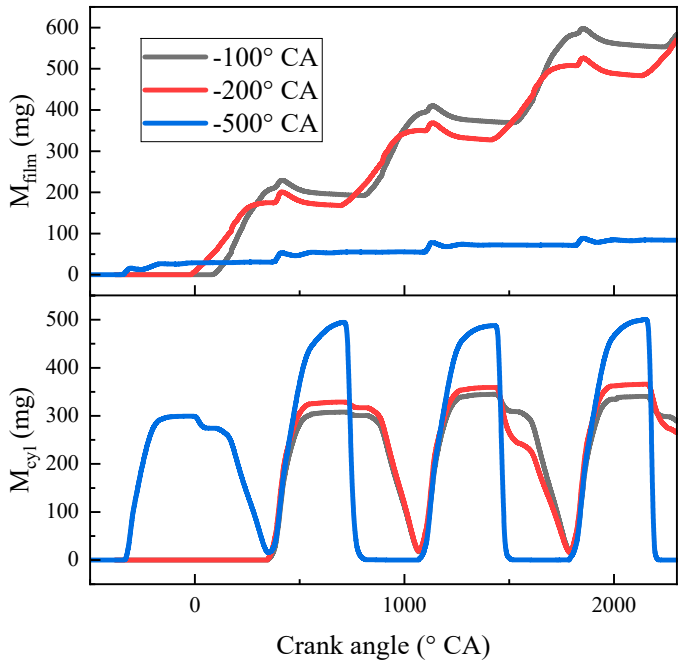


Figure 10. Evolution of methanol wall film mass (M_{film}) and in-cylinder mass (M_{cyl}) for 4 consecutive cycles under different injection timings.

Under the −500° CA condition, the wall film mass remains at an extremely low level with no significant accumulation (Figure 10), indicating good air-flow capability and minimal wall adhesion. In contrast, under the −200° CA and −100° CA conditions, the wall film mass shows a significant stepwise increase. This occurs because a large amount of fuel is injected onto the closed intake valve and port wall, hindering evaporation and leading to severe "wall-wetting." This substantial fuel retention not only causes fuel starvation in the current cycle but also reduces overall fuel utilization.

Furthermore, the in-cylinder methanol droplet distribution (Figure 11) visualizes the microscopic spatial distribution quality. Under the −500° CA condition, the turbulent intake airflow provides sufficient time for fuel atomization and mixing, resulting in a

uniform distribution of methanol droplets at the bottom dead center (BDC) and a homogeneous mixture favorable for flame propagation. Under the −200° CA condition, due to the short effective intake time, the number of fuel droplets entering the cylinder is scarce and unevenly distributed, with excessively lean local regions preventing the formation of a stable flame kernel. In summary, with long injection durations, adopting an early injection phase (e.g., −500° CA) to ensure effective overlap between the injection window and the intake stroke is a key strategy for suppressing methanol wall adhesion.

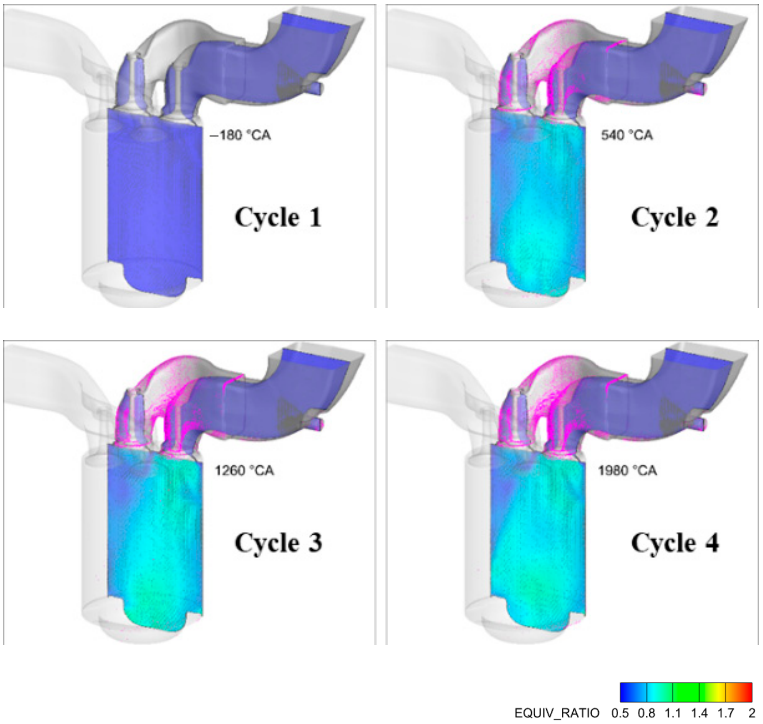


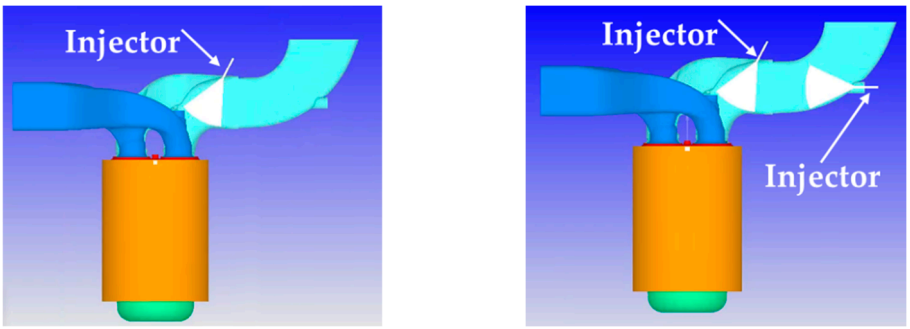
Figure 11. Spatial distribution of methanol droplets at the bottom dead center for four consecutive cycles with the injection timing of −200° CA.

Additionally, beyond mixture concentration and combustion stability, the injection strategy significantly affects the engine's knock tendency. Methanol possesses an extremely high latent heat of vaporization (approx. 1103 kJ/kg); rational utilization of this property is crucial for suppressing knock under high load or high compression ratio conditions. In the −500° CA SOI strategy (open valve injection), methanol enters the cylinder directly during the intake stroke or evaporates within the intake flow. This process absorbs substantial heat from the intake air and in-cylinder working fluid, significantly lowering the temperature at the end of intake and the start of compression. This "intake cooling effect" effectively lowers the in-cylinder mixture temperature at the end of the compression stroke, slows down the chemical reaction rate of the end gas, and prolongs the auto-ignition induction period, thereby playing a significant physical role in knock suppression.

Conversely, under the SOI strategies of −200° CA and −100° CA (closed valve injection), fuel mainly adheres to the intake port wall and the back of the intake valve. Here, the heat required for evaporation is derived primarily from the wall rather than the intake airflow. Although this cools high-temperature components, its contribution to reducing the in-cylinder charge temperature is minor. Thus, the closed valve injection fails to fully utilize methanol's latent heat to lower the charge temperature, leading to higher compression-end temperatures and thermodynamically weakening methanol's natural anti-knock advantage. Therefore, considering both cold start combustion stability and high-load knock suppression, the open valve injection strategy is superior.

3.3. Injector Number and Position

This section compares the impact of two injector installation positions. In the new position, the injector was placed significantly closer to the intake valve, and the injection orientation was directly toward the back of one intake valve (Figure 12a). The simulations maintained the start of injection at −500° CA and the duration of 513° CA.



(**a**) (**b**)

Figure 12. Schematic diagram of methanol injector positions: (**a**) new position; (**b**) dual-injector configuration combining original and new positions.

From the perspective of fuel transport, the change in injector position significantly alters the gas–liquid two-phase flow in the intake port. Comparing the port airborne droplet mass (M_{port}) and wall film mass (M_{film}) curves (Figure 13), it is evident that in the new scheme, the mass of suspended droplets decreases significantly while the wall film mass increases. This is attributed to the significantly shortened distance from the injector to the intake valve, which reduces the flight time and evaporation history of fuel droplets, causing them to impact the wall or valve back more easily under inertia. However, despite the increased wall film mass, the total fuel induction of the new injector position is superior to the original position in both cycles. This indicates that although shortening the injection distance sacrifices some pre-evaporation and spatial atomization, it effectively reduces fuel retention loss in the upstream intake port. This improves the transport efficiency of fuel entering the cylinder, especially during the intake valve opening phase, where fuel can be directly entrained into the cylinder.

Differences in mixture formation directly determine combustion quality. As indicated by the in-cylinder λ distribution (720–750° CA) in Figure 14, the original injector position results in large, excessively lean regions (light-colored) in the second cycle due to low fuel transport efficiency, which is unfavorable for flame kernel development. In contrast, the mixture concentration under the new injector position is significantly improved, forming a distribution close to the stoichiometric ratio or slightly rich (dark-colored) around the spark plug and in the main combustion chamber. This richer distribution lowers the minimum ignition energy required and significantly enhances flame propagation speed.

The comparison of combustion characteristics further confirms the improvement in mixture quality. The cylinder pressure and HRR curves show that in the first cycle, neither original nor new injector position forms effective combustion due to insufficient induction (black and red curves in Figure 15). However, in the second cycle, the new scheme demonstrates superior combustion performance: peak cylinder pressure increases substantially, and the HRR curve exhibits a high peak with appropriate phasing, indicating intense and sufficient combustion. The corresponding temperature field shows that the new injector position rapidly forms a large-scale high-temperature flame core after ignition, whereas in the original injector position, flame propagation is extremely slow due to the lean mixture, with high-temperature regions confined to the vicinity of the spark plug.

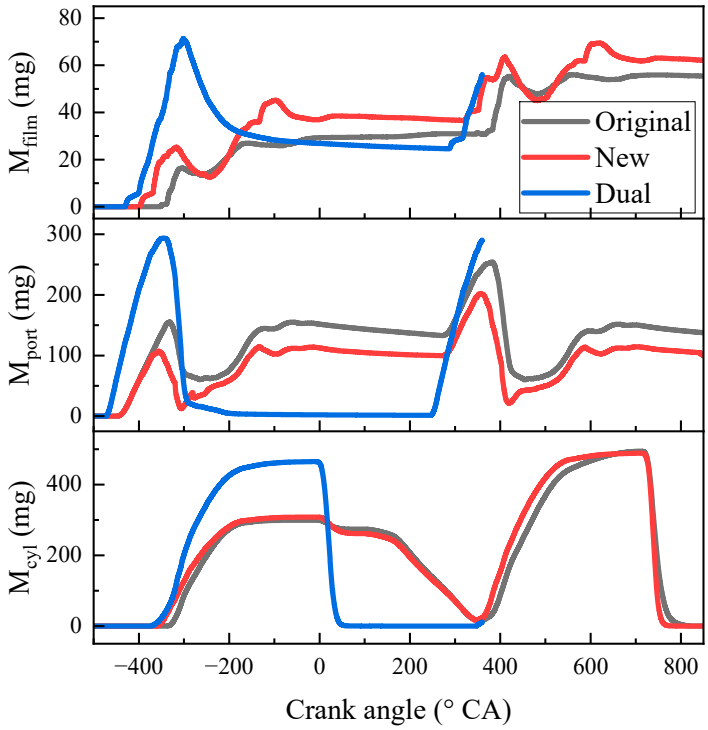


Figure 13. Evolution of methanol wall film mass (M_{film}), intake port mass (M_{port}), and in-cylinder mass (M_{cyl}) for 2 consecutive cycles under different injector positions.

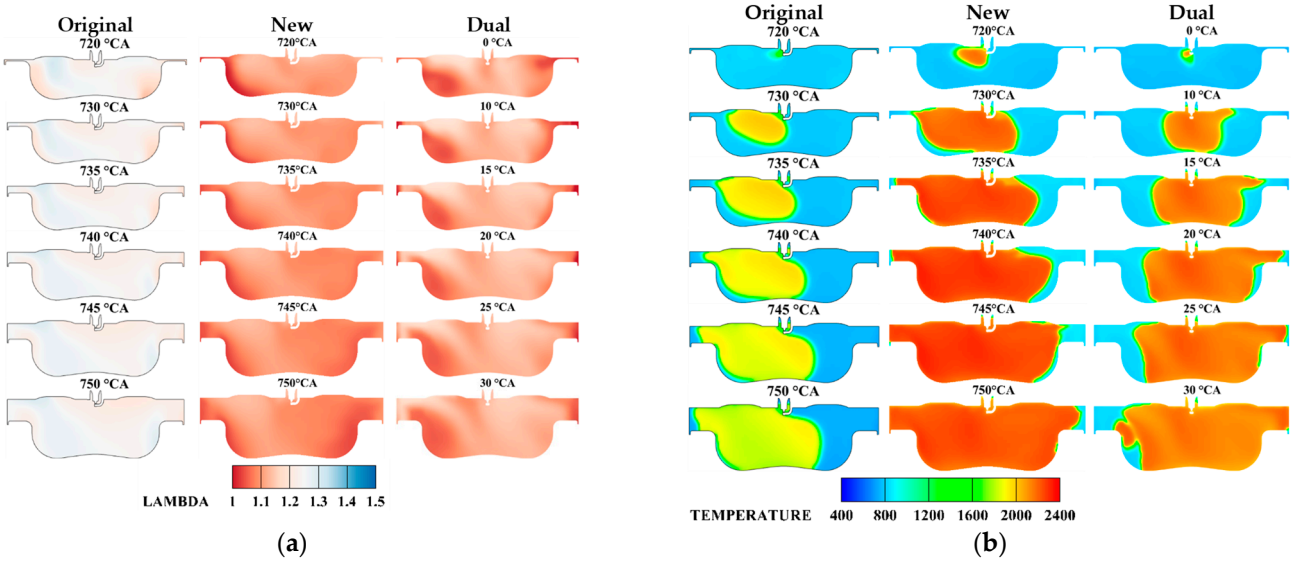


Figure 14. Distributions of in-cylinder λ and temperature under different injector positions: (**a**) λ; (**b**) temperature. The results for "Original" and "New" are from the 2nd cycle, while "Dual" is from the 1st cycle.

In addition to the new position scheme, a dual-injector configuration was analyzed. This configuration utilizes injectors at both aforementioned positions simultaneously, dividing the total injection duration equally between them while keeping the SOI at −500° CA. The numerical results show that this strategy produces a significant optimization effect (blue curve in Figure 15). The dual-injector configuration successfully balances the contradiction between fuel evaporation and transport efficiency. The upstream injector utilizes the longer flight distance to promote spatial atomization and pre-evaporation, reducing droplet diameter; meanwhile, the downstream injector utilizes its proximity to

the intake valve to quickly deliver fuel into the cylinder, compensating for the transport lag of the upstream injector.

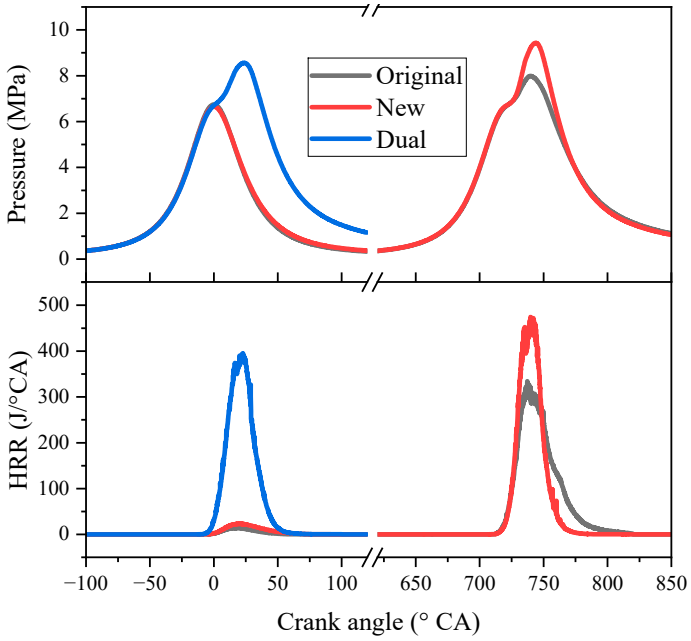


Figure 15. Cylinder pressure and heat release rate of consecutive cycles under different injector configurations.

Simultaneously, since the injection quantity of each injector is halved, the local wall film mass caused by the downstream injector is significantly lower than that of the single-injector (Figure 13), alleviating fuel loss due to severe wall-wetting. The in-cylinder λ distribution (Figure 14) shows that within the 0–30° CA range of the first cycle, a flammable mixture with a relatively uniform distribution close to the stoichiometric ratio (λ 1.1–1.2) forms in the cylinder. This stands in sharp contrast to the misfire situation caused by the overly lean mixture (λ > 1.5) in the two single-injector configurations during the first cycle. Consequently, the dual-injector configuration achieves strong combustion in the first cycle. The peak cylinder pressure exceeds 8 MPa, and the HRR peak is high and well-phased, demonstrating excellent stability. The evolution of the temperature field confirms that after ignition, the flame kernel forms rapidly and expands to the entire combustion chamber within the subsequent 20° CA.

4. Conclusions

In this study, a three-dimensional numerical simulation model of a methanol Port Fuel Injection (PFI) engine was established using the CONVERGE software. By coupling the detailed chemical kinetics with a calibrated wall film model, the research systematically investigated the dynamic equilibrium of fuel transport, the thermodynamic effects of injection phasing, and the spatial optimization of injector positions over multi-cycle operations. The specific conclusions are summarized as follows:

The formation of the in-cylinder mixture in methanol PFI engines is heavily governed by the “adhesion–evaporation” dynamic equilibrium of the intake port wall film. Due to methanol’s high latent heat of vaporization, a significant lag exists between fuel injection and fuel induction during the initial cycles. The simulations confirm that single-cycle calculations are insufficient; reliable performance prediction requires multi-cycle simulations to account for the gradual stabilization of wall film mass and air–fuel ratio. In standard

single-injector configurations, the first cycle often suffers from misfire or slow combustion due to severe wall-wetting and lean mixture conditions.

Injection phasing serves as a decisive factor for both fuel transport efficiency and knock suppression capability. The open valve injection strategy (e.g., SOI −500° CA) demonstrates distinct superiority over closed valve strategies (SOI −200°/−100° CA), achieving a 75% reduction in wall film mass. The long injection duration and early phasing allow the high-speed intake airflow to carry fuel directly into the cylinder, significantly minimizing wall film accumulation and avoiding the "fuel starvation" observed in closed-valve strategies. Open valve injection maximizes the "intake charge cooling" effect. By allowing methanol to evaporate directly within the intake air and cylinder, it significantly lowers the temperature at the start of compression. This mechanism effectively utilizes methanol's high latent heat, which is a potential way to suppress knock under high-load conditions.

Spatial arrangement of injectors involves a trade-off between atomization quality and transport speed. While moving a single injector closer to the intake valve improves induction efficiency by reducing upstream retention, it does not fully resolve transient response issues. The dual-injector strategy emerges as the optimal solution, which achieves a 66.7% increase in the fuel amount entering the cylinder compared with the original strategy. By simultaneously utilizing an upstream injector (promoting spatial atomization and pre-evaporation) and a downstream injector (minimizing transport lag), this configuration effectively balances the mixture formation process.

Author Contributions: Conceptualization, Z.D. and Y.Q.; methodology, X.X. and C.Z.; software, X.X. and Y.L.; validation, X.Z., K.S., and X.W.; formal analysis, X.Z.; investigation, X.X., Y.L., and K.S.; resources, Z.D. and Z.W.; data curation, X.X., Y.L., and K.S.; writing—original draft preparation, X.X. and Y.L.; writing—review and editing, Z.D., Y.Q., and Z.W.; visualization, X.X., Y.L., and K.S.; supervision, X.Z.; project administration, Z.D. and Z.W.; funding acquisition, Z.D. and Z.W. All authors have read and agreed to the published version of the manuscript.

Funding: This research received no external funding.

Data Availability Statement: The original contributions presented in this study are included in the article. Further details or requests for additional information can be directed to the corresponding author.

Conflicts of Interest: Authors Zhancheng Dou, Changhui Zhai, Xiaoxiao Zeng, Kui Shi and Xinbo Wu were employed by Weichai Power Co., Ltd. The remaining authors declare that the research was conducted in the absence of any commercial or financial relationships that could be construed as a potential conflict of interest.

References

1. Tian, Z.; Wang, Y.; Zhen, X.; Liu, Z. The Effect of Methanol Production and Application in Internal Combustion Engines on Emissions in the Context of Carbon Neutrality: A Review. *Fuel* **2022**, *320*, 123902. [CrossRef]
2. Verhelst, S.; Turner, J.W.; Sileghem, L.; Vancoillie, J. Methanol as a Fuel for Internal Combustion Engines. *Prog. Energy Combust. Sci.* **2019**, *70*, 43–88. [CrossRef]
3. Zhen, X.; Wang, Y. An Overview of Methanol as an Internal Combustion Engine Fuel. *Renew. Sustain. Energy Rev.* **2015**, *52*, 477–493. [CrossRef]
4. Gong, C.; Yi, L.; Zhang, Z.; Sun, J.; Liu, F. Assessment of Ultra-Lean Burn Characteristics for a Stratified-Charge Direct-Injection Spark-Ignition Methanol Engine under Different High Compression Ratios. *Appl. Energy* **2020**, *261*, 114478. [CrossRef]
5. Güdden, A.; Pischinger, S.; Geiger, J.; Heuser, B.; Müther, M. An Experimental Study on Methanol as a Fuel in Large Bore High Speed Engine Applications–Port Fuel Injected Spark Ignited Combustion. *Fuel* **2021**, *303*, 121292. [CrossRef]
6. Vancoillie, J.; Sileghem, L.; Van De Ginste, M.; Demuynck, J.; Galle, J.; Verhelst, S. Experimental Evaluation of Lean-Burn and EGR as Load Control Strategies for Methanol Engines. In Proceedings of the SAE 2012 World Congress & Exhibition, Detroit, MI, USA, 24–26 April 2012.

7. Li, Z.; Zhai, C.; Zeng, X.; Shi, K.; Wu, X.; Ma, T.; Qi, Y. Review of Pre-Ignition Research in Methanol Engines. *Energies* **2024**, *18*, 133. [CrossRef]
8. Shayler, P.J.; Colechin, M.J.F.; Scarisbrick, A. Intra-Cycle Resolution of Heat Transfer to Fuel in the Intake Port of an S.I. Engine. In Proceedings of the 1996 SAE International Fall Fuels and Lubricants Meeting and Exhibition, San Antonio, TX, USA, 14–17 October 1996; p. 961995.
9. Servati, H.B.; Yuen, W.W. Deposition of Fuel Droplets in Horizontal Intake Manifolds and the Behavior of Fuel Film Flow on Its Walls. In Proceedings of the SAE International Congress and Exposition, Detroit, MI, USA, 27 February–2 March 1984; p. 840239.
10. Li, Y.; Zhang, Z.; Liu, H.; Chang, W.; Shu, Z.; Wang, H.; Zheng, Z.; Zhao, H.; Wang, X.; Yao, M. Experimental and Simulation Study on Reducing the Liquid Film and Improving the Performance of a Carbon-Neutral Methanol Engine. *Energies* **2025**, *18*, 353. [CrossRef]
11. Yuan, B.; Zhang, X.; Cao, J.; Wang, L.; Wang, Z. Investigation on the Development Law of Methanol Spray Impinging on Intake Valve during Port Fuel Injection. *Energy* **2025**, *320*, 135250. [CrossRef]
12. Wang, Q.; Wang, B.; Yao, C.; Liu, M.; Wu, T.; Wei, H.; Dou, Z. Study on Cyclic Variability of Dual Fuel Combustion in a Methanol Fumigated Diesel Engine. *Fuel* **2016**, *164*, 99–109. [CrossRef]
13. Chen, Z.; Yao, C.; Yao, A.; Dou, Z.; Wang, B.; Wei, H.; Liu, M.; Chen, C.; Shi, J. The Impact of Methanol Injecting Position on Cylinder-to-Cylinder Variation in a Diesel Methanol Dual Fuel Engine. *Fuel* **2017**, *191*, 150–163. [CrossRef]
14. Mousavi, S.M.; Tripathy, S.; Molander, P.; Dahlander, P. Effects of Port-Fuel Injected Methanol Distribution on Cylinder-to-Cylinder Variations in a Retrofitted Heavy-Duty Diesel–Methanol Dual Fuel Engine. *Fuel* **2025**, *391*, 134733. [CrossRef]
15. Liu, H.; Yan, Y.; Jia, M.; Xie, M.; Lee, C.F. Three-Dimensional Numerical Investigation on Wall Film Formation and Evaporation in Port Fuel Injection Engines. *Numer. Heat Transf. Part A Appl.* **2016**, *69*, 1405–1422. [CrossRef]
16. Yuan, B.; Wang, Z.; Cao, J.; Huang, Y.; Shen, Y.; Song, Z.; Zhao, H.; Cheng, X. Mixture Formation Characteristics and Feasibility of Methanol as an Alternative Fuel for Gasoline in Port Fuel Injection Engines: Droplet Evaporation and Spray Visualization. *Energy Convers. Manag.* **2023**, *283*, 116956. [CrossRef]
17. Li, J.; Gong, C.-M.; Su, Y.; Dou, H.-L.; Liu, X.-J. Effect of Injection and Ignition Timings on Performance and Emissions from a Spark-Ignition Engine Fueled with Methanol. *Fuel* **2010**, *89*, 3919–3925. [CrossRef]
18. Zhu, Z.; Mu, Z.; Wei, Y.; Du, R.; Guan, W.; Liu, S. Cylinder-to-Cylinder Variation of Knock and Effects of Mixture Formation on Knock Tendency for a Heavy-Duty Spark Ignition Methanol Engine. *Energy* **2022**, *254*, 124197. [CrossRef]
19. Wei, Y.; Zhu, Z.; Liu, S.; Liu, H.; Shi, Z.; Zeng, Z. Investigation on Injection Strategy Affecting the Mixture Formation and Combustion of a Heavy-Duty Spark-Ignition Methanol Engine. *Fuel* **2023**, *334*, 126680. [CrossRef]
20. Tian, Y.; Zhu, J.; Li, W.; Li, W.; Xing, Y. Effect of Injection Angle on Combustion and Emission Performance of Spark Ignition M100 Methanol Engine in Equivalent Combustion. *Energy* **2025**, *324*, 135876. [CrossRef]
21. Wen, H.; Yu, Y.; Li, J.; Xu, C.; Jing, H.; Shen, J. Numerical Investigation on the Influence of Injection Location and Injection Strategy on a High-Pressure Direct Injection Diesel/Methanol Dual-Fuel Engine. *Energies* **2023**, *16*, 4518. [CrossRef]
22. Chen, W.; Yang, X.; Zuo, Q.; Wang, H.; Ning, D.; Kou, C.; Zhang, Y.; Zhu, G. Combustion Characteristics and Performance Analysis of a Heavy-Fuel Rotary Engine by Designing Fuel Injection Position. *Appl. Therm. Eng.* **2024**, *247*, 123021. [CrossRef]
23. Chang, W.; Wang, C.; Wu, Y.; Jin, C.; Zhang, Z.; Liu, H. Study on the Mechanism of Influence of Cetane Improver on Methanol Ignition. *Fuel* **2023**, *354*, 129383. [CrossRef]

Disclaimer/Publisher's Note: The statements, opinions and data contained in all publications are solely those of the individual author(s) and contributor(s) and not of MDPI and/or the editor(s). MDPI and/or the editor(s) disclaim responsibility for any injury to people or property resulting from any ideas, methods, instructions or products referred to in the content.